

FINAL REPORT

to

JOINT OCEANOGRAPHIC INSTITUTIONS, INC.

on

"Reprocessing of Multi-channel Seismic Data off
Guatemala for an IPOD Transect"

(JOI-UTMSI P. O. NO. 25, IPOD TRANSECT LEG 84)

(GMGL 26-7601-54XX)

from

Dr. Ian Norton, Institute for Geophysics,
The University of Texas at Austin
(now of Exxon, Inc.)

Dr. Roland von Huene, U.S. Geological Survey

Dr. John Ladd, Lamont Doherty Geological Observatory

15 March 1982

Under a contract from JOI, seismic data collected by the University of Texas Marine Science Institute in 1977 and 1978 off Guatemala was reprocessed to clarify geology features required to meet the OMD objectives, to satisfy the JOIDES Safety Panel, and to site holes for Leg 84. In all, 20 records were rescaled, filtered, and run at various gain settings as the first primary data set. Restacking was required on 3 records. Four records that had not been previously processed were brought to the basic processing level of the whole survey.

Certain prime records were processed further to enhance the basement reflections or give better resolution in slope deposits. Wavelett processing was used in one line and 4 lines were migrated.

All of the above records were microfilmed and printed by xerography or were printed photographically on milar film. A set of microfilms has been sent to the IPOD data bank at LDGO.

Some initial results from the reprocessed seismic data were the basis of the attached report to be published in Volume 67 of the Initial Reports of the Deep Sea Drilling Project.

11/7/91 FIRST
MANUSCRIPT
for Leg 67
Initial Report

SOME GEOPHYSICAL OBSERVATIONS IN SLOPE DEPOSITS
OF THE MIDDLE AMERICA TRENCH OFF GUATEMALA

by

Roland von Huene, U. S. Geological Survey
John Ladd, Lamont-Doherty Geological Observatory
Ian Norton, University of Texas, Galveston

ABSTRACT

Slope deposits drilled during Leg 67 were detailed in redisplayed seismic records after the leg. These deposits are of significantly lower seismic velocity and probably lower density than the underlying basement to indicate a contact between rocks of differing consolidation and not a continuous sedimentary sequence. The slope deposits cover basement terranes of 3 different topographies. The shelf edge is an arch whose seaward flank forms a steep (up to 15°) upper slope. The mid-slope area has a rugged topography covered by thick slope deposits. The lower slope is relatively smooth except where broken locally by benches. The upper and middle slope areas are associated with strong magnetic anomalies and rare landward dipping reflections truncated by the rough surface. We explain the rough mid-slope topography by subareal erosion succeeding the first uplift of this area in the Paleocene and prior to major subsidence in the early Miocene. The present slope deposits then covered the trench landward slope, perhaps coincident with the increased arc volcanism indicated by ash layers, and thus the present period of subduction.

The subducted ocean crust has a distinct linear topography of hundreds of meters relief that seems to disappear beneath the landward slope of the trench along with most of the ocean basin and trench sediment. The almost passive

assimilation of oceanic material without significant accretion in the late Neogene argues for significant decoupling at the front of the subduction zone.

A base of gas hydrate reflections can be identified in many of the redisplayed seismic records off Guatemala. Base of hydrate reflections are most common where slope deposits are thick and the reflections have not been identified in the underlying acoustic basement. This is consistent with the geochemical evidence that gas hydrate has its source in the organic rich slope sediment. The hydrate depth and temperature measurements in drill holes indicate a temperature gradient similar to that measured across the Japan Trench.

INTRODUCTION

In preparation for the IPOD drilling of the Middle America trench transect off Guatemala, a gridded network of geophysical observations was made by the University of Texas that included seismic refraction, seismic reflection, magnetic, and bathymetric measurements. A post Leg 67 survey was made by CONEXO with SEABEAM. These studies are summarized individually in companion papers (Ladd et al, Aubouin et al, this volume). The IPOD and some earlier surveys were made to study, the deep structure of the arc-trench system concentrating on the refraction crustal velocity structure (Shor and Fisher, 1961; Ibrahim et al., 1979), the crustal structure as modeled from gravity and magnetic observations (Couch and Woodcock, 1981), and the configuration of deep seismic reflections (Seely et al., 1974; Ladd et al., 1978; Ladd et al., this volume). Most of the IPOD drilling, however, did not penetrate to the horizons significant in the crustal geophysical studies. In this paper we emphasize a study of the geophysical data from the sea floor to

a depth of 2-4 km through re-examination of seismic reflection records, most of which have been scaled and re-displayed using parameters that emphasize the shallow structure and particularly any reflections developed on the base of the gas hydrate zone. Some of the new discoveries during Leg 67 have prompted examination of features such as gas hydrate which were not investigated in earlier studies. Through this study we have reconciled some of the differences between interpretations of the geophysical data made prior to drilling, and the interpretation of data from the Leg 67 core.

SEISMIC CHARACTER OF SLOPE SEDIMENT

Velocity

Seismic velocity was measured in 3 ways, first on the core aboard the Challenger with a Hamilton frame (Boyce, 1976), second in making the normal moveout correction during processing of the seismic reflection data, and third with the refraction measurements. Velocity measurements on the core from Site 494 gave an almost constant value of 1.7 km/sec in slope deposits and values of 3.5 to 4.0 from underlying sedimentary and igneous rock. At site 496 and 497 velocity measurements were difficult to make because of the amount of entrained gas but when a value of 1.6 km/sec was assumed, the features in seismic reflection records correlated well with those penetrated by the drill.

The velocities of slope sediment indicated by semblance analysis are generally between 1.5 and 1.7 km/sec (Ladd et al., this volume). When the base of the slope sediment is well defined, the semblance analysis generally indicates a nearly constant velocity value in the first 500 m of slope deposits and then a very rapid increase in the underlying rock.

In seismic refraction measurements the uppermost units have velocities from 1.8 to 2.5 km/sec (Shor and Fisher, 1961; Ibrahim et al., 1979). Some of these velocities are too high for slope deposits and are instead derived from the interface at or below the base of the deposits, as defined in the reflection data. The thinness, the irregular bedding, and the roughness of the base of the slope deposits commonly makes these refraction measurements difficult. In 3 refraction stations, velocities of 1.6 to 2.0 km/sec were obtained from horizons clearly within the slope deposits (Stations 1, 3 and 8, Ibrahim et al., 1979). Within the zone of coherent reflections at the base of the slope deposits, refraction velocities are from 2.0 to 2.1 km/s, and immediately below the slope deposits they range from 2.3 km/sec to 3.3 km/sec. The 3 types of measurements indicate that the velocity contrast between slope deposits and the underlying rock which forms an acoustic basement* can be relatively large resulting in reflection coefficients, particularly if the contrasting units are in sharp contact. This situation should result in the strong reflections at the base of the slope deposits which are observed in the seismic records. At the other extreme are areas with no strong reflection at the base of the slope deposits which may result from a low velocity contrast, a complex contact, or a depth of burial great enough to mute the seismic expression of the base of the slope deposits.

*"Acoustic basement" in the seismic reflection records has 2 meanings. If it represents the interface between rocks added to the edge of the continent that now form the leading edge of the continental framework, and sediment of the overlying slope deposits we refer to the surface simply as basement. This usage does not imply continental, intermediate or other types of crustal structure. When "basement" is used to denote the top of the igneous oceanic crust it is prefaced with "oceanic".

Identification of basement

Acoustic basement at the base of the slope deposits is commonly an irregular surface associated almost everywhere with diffractions (Fig. 2). These diffractions have at their crests a very high amplitude and are of a frequency lower than the overlying reflections. The sharpest contact between basement and slope deposits is a single diffractive reflection but more often multiple overlapping diffractions are seen.

The first criterion we used to identify the base of the slope deposits is high reflection amplitude which are probably the result of the general contrast in velocity and/or density between slope deposits and underlying rock. Secondary criterion are a diffractive character and a general continuity of reflection in slope deposits and lack of continuity in the underlying rocks. The boundary chosen could easily be shifted by 1 or more phases because only rarely is the contact sharply displayed. The diffuse nature of the contact is probably as much a function of recording multiple events from within and outside of the plane of section as it is a function of a complex or gradational boundary. The amplitude of the reflection is commonly as great or greater than the reflection at the seafloor, despite its depth at 0.5 km to 1 km, which would not be the case if a broadly gradational velocity increase marked the boundary. As indicated previously, the velocity increase at the base of the slope deposits can be 0.6 km/sec to perhaps as large as 3.0 km/sec whereas the increase at the seafloor is about 0.2 km/sec. We have little control on density but a similar shift in rock density would be expected. The amplitude criterion, however, sometimes breaks down, especially on the lower slope, and locally it cannot be applied without some consideration of reflection continuity and structure. Thus, the

interpretation of basement depth is locally very uncertain.

Nature of the base of the slope deposits surface

The broad morphology of the base of slope deposits surface, is also reflected in a subdued way in the topography of the trench slope (Fig. 3). Overall, the seafloor topography of the trench slope falls 6 km in about 60 but its uppermost 2000 m generally consist of a steep slope, the next 1000 m are the least steep, and the lower 2000 m are commonly a steep nearly planar surface marked locally by step-like benches. A large transverse canyon, San Jose canyon, has deeply incised the sedimentary sequence at the edge of the shelf and the upper slope but the canyon becomes obscure on the lower slope. and indistinguishable from the numerous smaller canyons that traverse all parts of the slope.

The gross topography of the basement (Fig. 4) is divided into: 1) an initial steep (avg. 12°) 1.5 km drop-off at the edge of the continental shelf and beneath the upper slope, 2) an area with gentle dip (avg. 2°) and local relief as large as 1 km, in the middle slope, 3) a lower slope of moderate dip (avg. 5°) and generally smooth except where cut by a series of descending benches. A generalized topography of the basement surface (Fig. 5) indicates the rough topography of the mid-slope as contrast to the smoother topography of the upper and lower slopes.

The relation of bedding the basement to the basement surface is apparent locally. Parts of the surface have truncated faint bedding which can be seen on records trending both parallel and perpendicular to the slope. Landward dipping layers deep in the continental framework have been emphasized by Ladd et al (this volume) on record GUA-13 and are also suggested by Seely et al,

(1974). These layers are truncated at the basement surface, especially in the mid slope area. Along portions of records paralleling the upper slope, bedding in the basement locally conforms to the base of slope deposits surface as well. Truncation of beds by massive erosion is clearly seen in upper San Jose canyon (Fig. 6), however, here the basement surface is covered by sediment filling the canyon and thus a probable product of multiple stages of erosion and deposition. Elsewhere the truncation is not so clearly defined. In general, the origin of the basement surface, whether by tectonism or erosion, is unclear.

Reflection character in slope deposits

Bedding within the slope deposits is best resolved along the upper slope and the resolution degrades progressively down slope as the distance of reflectors from the seismic source and receiver increases. In the middle slope area of relatively gentle dip, maximum slope deposit thickness in troughs are about 1 km (1.3 km/sec). Reflections are sometimes continuous for 7 km in lines parallel to the slope. At the other extreme are areas without many coherent reflections. On the lower slope of the trench, a uniform cover of diffractive short reflections is most common, and little sedimentary structure can be determined.

Structure in the middle slope where sediment has collected most rapidly shows local thin reflective sequences conforming to the basement surface, often of only 1 or 2 reflections of high frequency. More commonly, the reflections lap onto, or abut, the rough basement surface, or a general zone of seismic "hash" covers basement. Above the basal zone is one where reflections are configured in patterns commonly identified as lobate

(deltaic?), as fine overbank strata, and as ponded sediment. The record clarity is insufficient to make good estimates of the amount of sediment transported by the various processes as is indicated in the rare, clearly configured examples. This is in part due to the lack of velocity contrast in the section as shown by the general low amplitude-high frequency reflections which is consistent with the muddy section that was drilled. A seismic system with a greater band width than used in this study might better resolve structure within slope sediments.

STRUCTURE IN SLOPE DEPOSITS

AROUND THE LEG 67 DRILL SITES

The preceding provides a general background for the more specific description of seismic reflection records at 2 groups of drill sites. The following interpretations supercede those in the site chapters since the interpretation here is based on seismic displays not available during preparation of the chapters.

Sites 496 and 497, upper slope

At these sites the landward dipping reflection described by Ladd et al (this volume) was the main objective, but it was not reached because of the intervening gas hydrate (von Huene, Aubouin et al, 1980). An expanded, re-stacked, and re-scaled section of seismic record GUA-13 (Fig. 7) indicates penetration at Site 496 of a hemipelagic slope section onlapping a lobate body that downlaps the basement surface above the landward dipping reflection. Cutting the lower unit is a base-of-gas-hydrate reflection. Drilling at Site 496 penetrated first a unit of biogenic mud and at the unconformity (0.25 sec

deep) it went through a thin mud unit with very slow relative rates of sediment accumulation and then into a semilithified sandy mudstone of Miocene age. Both the upper and lower units have abundant terrigenous detritus, volcanic ash, and rare lignite.

Another seismic record (not shown here) crossing at the site but perpendicular to GUA-13 shows a 5 km wide low mound of sediment with overlying strata lapping onto it. The overlying strata are part of the fill of San Jose Canyon. It is not clear whether the lobate sediment body is part of an ancient canyon fill or part of the material deformed and then eroded by the canyon. The initial age of canyon cutting, is thought by Ladd and Schroder (this volume) to have perhaps started in the lower Miocene or upper Oligocene. The lobate sediment body is of lower Miocene age (Site 496, this volume).

Drilling at Site 497 is just seaward of figure 7 and penetrated an equivalent of the upper unit. The correlations of seismic strata between these 2 sites was unclear in the original display of GUA-13 and in the Glomar Challenger records because of the overlapping diffracted reflections from basement and the gas hydrate.

The seismic and drill data indicate that at Sites 496 and 497, a hemipelagic slope sequence of Quaternary and Pliocene age covered a lobate body of early Miocene age, probably a fan. This probable fan contains sediment deposited in neritic water depths (Thompson, this volume) that was out of the path of rapid slope sedimentation during middle and part of late Miocene time, perhaps because it stood above the surrounding slope. The fan may have been associated with an early equivalent of San Jose Canyon that was later incised, as the shelf break structure grew, but this speculation is

essentially untested without better resolution in the seismic data.

Sites 494 and 498, lower slope

These sites, on the lowest of the sequence of benches on the lower slope of the trench, were drilled to penetrate from the upper to the lower plate in a subduction zone. Hole 494 was terminated because of bit failure, and at hole 498 gas hydrate caused termination. Why was there such a difference in the section at 2 holes only 1.7 km apart?

Very little can be read in the part of record GUA-13 across Site 494. Record GUA-9 (Fig. 8) in a perpendicular direction shows the base of the slope deposits better. It has been proposed that Site 494 was drilled on a high in the surface at the base of the slope deposits whereas 498 was not (von Huene, Aubouin, et al, 1980). But this explanation cannot be varified by the seismic data in view of the uncertainties in position of the drill sites to the high seen in record GUA-9. The highest part of a large hump in GUA-9 is not directly below Site 494 nor is the lowest part beneath Site 498, but without 3 dimensional migration the hump cannot be positioned correctly with respect to the sites; the location of the track lines is also not known much better than 1 or 2 km.

Topographic relief is also seen on the subducted igneous ocean crust, the basement, which appears locally in records along the base of the slope as a ringing sequence of low frequency reflections (line GUA-2, Ladd et al, this volume, fig. 7). The relief in record GUA-2 is of the same general height and width as the relief across the horst and graben topography in the seaward slope of the Middle America Trench. As the ocean floor is flexed downward into the trench, ridges of 200 m to 500 m height are formed. A vertical

relief of 400 m is common on the subducted ocean crust although once deeply buried in the subduction zone the higher velocities of the overlying rocks and other acoustic effects subdue the apparent height of ridges and valleys in time sections. Seismic records paralleling the slope also show basement relief some being concordant and other being non-concordant with the overlying topography of the ocean floor. The relief is difficult to observe because the basement is best recorded where it is flat and does not scatter or diffract seismic energy. The reflections are of low amplitude and were obscured in some processing steps such as deconvolution.

In two records, coherent reflections from sediment layers appear over the basement reflections (Fig. 8). Some of these reflections probably indicate layers of coherent subducted sediment. Sediment subduction is required by the lack of a modern accretionary complex around Site 494.

Record 9 crosses Site 494 (Fig. 1) and continues west along the base of the slope. The coherent flat reflections below a highly diffracted seafloor reflection (Fig. 8) could be from the trench floor out of the plane of section, or they could be from a buried coherent sediment sequence. The reflections appear suspiciously strong for strata buried about 500 m beneath the trench landward slope.

Record 8 along the base of the slope, but in the eastern part of the surveyed area, also shows apparently buried coherent reflections above the basement (Fig. 8). These reflections seem more likely to be from subducted sediment because they are from 0.8 to 1.1 sec. below the seafloor as opposed to 0.5 sec. in the previous record and appear more concordant with the basement structure. They occur beneath relatively gentle topography and simple structure where seismic energy is not scattered.

GEOPHYSICAL EVIDENCE OF GAS-HYDRATE

Since the first encounter of gas-hydrate in the core from Site 496, a renewed effort was made to find bottom simulating reflections that would indicate the base of gas hydrates (Shipley et al, 1979). Shipley had informally noted a possible gas-hydrate in GUA-14 prior to drilling, but the evidence in other records was not convincing. Subsequent to Leg 67, an expanded display of the GUA-14 traces was made which showed a polarity reversal of the BSR as compared with the seafloor polarity (Fig. 9), the expected response to a reflection from the interface of a high-velocity hydrate over a low-velocity gas charged sediment (Ladd et al, this volume).

The seismic records were re-displayed with scaling factors that enhanced the BSR's and the structure of slope deposits, (short AGC window, no variable gain and no filtering of high frequency data). The depths of all BSR's recognized in the new seismic displays (Fig. 1) were plotted at 2.5 km intervals with BSR's from other areas with recognized hydrate reflections (Shipley et al 1979). The field of points from Guatemala fits the field of the base of hydrated zone well (Fig. 10). Parts of two Guatemala BSR's do not fall within the field shown for Guatemala. This is explained as follows. A constant velocity of 1.7 km/sec was used to convert time information to depth. This velocity is inappropriate for the lobate sediment bodies, including the one in figure 7. These lobate bodies are probably fans and contain more sand than the slope sediment as was shown by the drilling at Site 496. Unfortunately no velocity log was run at Site 496, but if a velocity of 1.8 km/sec to 1.9 km/sec is used to determine depth of the BSR, these points fall within the field shown in figure 10. The points are not necessarily inconsistent with the gas hydrate stability curve but they are poor points to

use in a test for gas hydrate.

Within the Guatemalan field are points from about 100 line km that were recognized in the re-displayed seismic records (Fig. 1). From the correspondence between Guatemalan hydrate depths and those from other areas, and from the polarity reversal test, it is assumed that the BSR is a base of gas hydrate reflection and not a diagenetic boundary.

The gas hydrate BSR's are concentrated in the mid-slope area. They tend to be locally developed and are generally 100 m or more above the base of thick slope deposits (Fig. 11). This is consistent with the proposed origin of the hydrated methane gas from the 2% to 5% herbaceous material in the slope deposits. Samples of rock below the slope deposits at Site 494 have low concentrations of organic carbon, which may explain the absence of gas hydrate BSR's in areas of thin slope sediment.

From the gas hydrate BSR's, temperature at the base of the hydrate zone was estimated by using the solid/gas phase relation of the methane gas hydrate system. These temperatures and depths, (Table 1) and the temperature at the water/sediment interface, gave a temperature gradient that could be compared with temperature gradients from Leg 67 drill holes and unpublished temperature data from the Petrel #1 well (Fig. 12). The base of gas hydrate derived values have a maximum scatter of about 5° C/km and average 30° C/km. The temperature sensor left in hole 494A which came to thermal equilibrium through 6°C in about 10 days gives a value of $22 \pm 5^\circ$ C/km (von Huene, Aubouin et al, 1980). If the single temperature value logged at Site 497 is corrected for drilling effects by adding the $6 \pm 1.5^\circ$ C change from drilling measured at Site 494 (drilling histories were similar), it falls at the upper range of the gas hydrate derived temperature field. The temperature gradient in the upper

500 m of the Petrel #1 (Fig. 13) has a broad range of uncertainty if the shallowed determinations at 447 m are accepted but this reading was probably affected most by drilling.

The temperature gradients derived from gas hydrate data are very consistent with those from the bottom hole data (Fig. 12). There appears to be a gradual increase in temperature gradient landward as has been observed in heatflow data including DSDP drill holes on the Japan trench convergent margins (Burch and Langseth, 1981).

DISCUSSION

In a companion paper, Ladd et al (this volume) discuss the deep geophysical evidence for landward dipping slabs of possible oceanic material beneath the slope of the Middle America Trench off Guatemala. They conclude that slices of oceanic material may form an imbricated complex as first proposed for this area by Seely et al (1974). Imbrication in the Paleocene or earliest Eocene is dated by the uplift of a section penetrated in the Petrel well (Seely, 1979). Seely (1979) shows an unconformity at the edge of the shelf associated with the Paleocene uplift and a subsequent Oligo-Miocene unconformity as well. A greater angular discordance is seen across the Oligo-Miocene unconformity than across the Paleocene one indicating strong tilting of forearc strata at the present shelf edge (Ladd and Schroder, this volume). The truncation of middle and late Eocene beds by the Oligo-Miocene unconformity also indicates subaerial erosion at the shelf edge and Seely (1979) infers forearc basin subsidence and lowering of sea level as the principal cause of this unconformity. We build on this background in interpreting some of our data and developing more detail in the tectonic history.

At Site 496 in 2064 m of water the inferred fan deposits contain fauna of early Miocene age from shelf depths. The 2000 m or more depth difference since the early Miocene is larger than the postulated 500 m change in sea level for this period (Seely, 1979) indicating subsidence of the mid-slope area. Subsidence of the forearc basin also occurred in the early Miocene (Seely, 1979); therefore arching of the shelf break and subsidence of both the seaward and landward flanks is indicated. The landward flank seems to have been tilted more in the early Miocene than in the Paleocene because the angular discordance appears largest across the Oligo-Miocene unconformity in the seismic records (Seely (1979)). The probable shallow water delta now beneath the slope sediment of the middle and upper slope is tectonically significant in showing Miocene arching of the shelf edge, and in indicating the Miocene time of initial slope sediment deposition. Similar deltaic structures are seen in the slope deposits not only in the area of San Jose Canyon where such deposits were drilled, but also near seismic lines 11 and 15 in the mid-slope area where there are no comparable large present canyons. Thus a major tectonic event affected the present shelf edge in early Miocene time in addition to the Paleocene uplift.

The deltaic deposits of early Miocene age lap down onto the underlying rocks of the continental framework and suggest that the mid-slope was first covered by slope deposits in the early Miocene. The first slope deposits are also of early Miocene age at Site 494 (Scientific Staff, this volume). If these ages from the lower and mid-slope areas are typical, the present bed rock framework of the trench slope has existed since the early Miocene. From the two points of age control there is no evidence for progressive imbrication and uplift through the Neogene as was developed along the Middle America

Trench off southern Mexico (Moore, Watkins et al, 1979). However, an absence of Neogene imbrication is consistent with the lack of a Neogene accretionary complex at Site 494.

If not accretion and imbrication, what are the subduction related tectonic processes that have structured the landward slope of the trench off Guatemala during the Neogene? This question has no very satisfactory answer in the existing data but some puzzling information on modern structure is seen beneath the lower slope where the subduction zone is shallow.

The ocean crust entering the subduction zone has a horst and graben topography of up to 700 m vertical relief, formed as the crust is flexed downward along the seaward side of the trench. SEABEAM mapping shows that rather than trending parallel to the trench, the horst and graben strike 35° from the trend of the trench axis (Aubouin et al, this volume). If subduction of a high ridge or deep trough on the lower plate deforms the upper plate, these effects should be marked by an oceanic topographic trend superimposed on the trench landward slope. A subdued oceanic topography from subduction of ocean crust relief should be most obvious at the thin leading edge of the upper plate or atleast at the base of the trench landward slope.

Surprisingly, the SEABEAM map shows an abrupt termination of the two completely mapped ridge and trough pairs at the foot of the trench landward slope. Yet seismic reflection records show relief on the subducted igneous ocean crust suggesting that much relief of the oceanic basement is not sheared off. Unfortunately the seismic records are insufficient to show whether the 2 ridges on the SEABEAM map continue beneath the landward slope of the trench. Although the horst and graben relief is subdued by sediment ponded along the trench axis, the rate of sediment accumulation is insufficient to bury the

ridges completely (Sites 499 and 500, Scientific Party, this volume). If the 2 ridges do not end fortuitously at the trench axis, then much of the deformation from subduction of basement features that are hundreds of meters high is decoupled somewhere below the slope deposits in a zone that is locally less than 1 km thick. Even if the ridges end, many other ridges must have been subducted. If the present rate of subduction (10 cm/yr) has existed for 15 MY, and the 10 km spacing of ridges and troughs in the SEABEAM map is representative of the subducted topography, then at least 150 ridges and troughs have been subducted without imparting a diagonal trend on the slope topography. The short sections of the benches at the base of the slope that are mapped with the SEABEAM are subparallel to the trench axis and do not reflect the horst and graben trend. Their appearance on seismic records suggests collapse features (Ladd et al, this volume, fig. 5) but their subsurface structure is poorly defined in the records.

The partially mapped eastern ridge on the SEABEAM map (Aubouin et al, this volume) may have shaped the trench lower slope where the foot of the slope and the ridge collide. The topography from the UTMSI bathymetric records show a possible change in trend of the trench axis parallel to the horst and graben topography at the point of collision (Fig. 3, point A). Thus the subduction of the horst and graben topography seems to be both passive and active. However, it appears that the upper and lower plates are highly decoupled.

The subduction of horst and graben must certainly facilitate the subduction of sediment which is consistent with the seismic evidence of unbroken strata on subducted igneous ocean crust. A form of tectonic erosion by gross abraision from horst and graben has been proposed by Hilde (1978) and

by Schweller and Kulm (1978). Yet, the apparent weak coupling across the subduction zone seems at odds with a mode of subduction erosion where large blocks are forcefully abraided.

TECTONIC HISTORY

The tectonic history of the Middle America trench off Guatemala probably involves imbrication during the Paleocene as proposed by Seely et al (1974), and emphasized by Ladd et al (this volume), but periods where other subduction related tectonic mechanisms were dominant are required to explain the drilling and geophysical observations. This is particularly true along the upper and the mid-slope area of rough topography, of local magnetic anomalies, of strong truncated landward dipping reflections and of subsidence. We speculate here to account for the rough topography, the truncation, and the subsidence by proposing subaerial erosion in the period between the Paleocene uplift and the early Miocene, followed by arching at the present shelf edges. In early Miocene the first fans were deposited on the middle and upper slope and some were perhaps associated with an ancestral San Jose Canyon, which has deeply eroded the shelf edge arch. Perhaps the area which San Jose Canyon cut to depths of as much as 1 km was part of subaerial terrane and the lower and less prominent reaches of the canyon were submarine. Similarly, the rough mid-slope topography might be an extension of the erosion surface along the arch not only to explain the topography but also because the middle and upper slopes have sediment that was deposited at shelf depth. Unfortunately, the spacing and resolution of our seismic data are insufficient to define any buried drainages or other indication of subaerial erosion. As Seely (1979) and Ladd et al (this volume) have noted, the magnetic anomalies are probably from

intrusions or slices of igneous oceanic crust truncated by the erosion surface. Perhaps during the early Neogene a terraine similar to that of the Nicoya Peninsula existed along the upper slope which then subsided. On the landward side of the shelf edge arch there was subdidence in the forearc basin. During the early Miocene the tempo of explosive volcanism was higher than in most of the Neogene (Cadet, this volume, Kennet et al, 1977). Thus, after major tectonism in the early Paleocene (Seely, 1979), when the Nicoya, Santa Elena and other terranes may also have been assembled (Azema, this volume), the margin off Guatemala experienced strong early Miocene tectonism associated with subduction and the rock of the present continental framework took on enough of its present structure to allow deposition of the Neogene slope deposits.

The present tectonism involves subduction of considerable sediment, probably facilitated by the seemingly passive disappearance down the subduction zone of ridges hundreds of meters high. This suggest extensive decoupling across the front of the subduction zone, although the communication of tectonic stress may be sufficient to produce locally recognized deformation near the ocean floor.

FIGURE CAPTIONS

- Figure 1. Ships tracks of multichannel seismic reflection records made in 1977 by the University of Texas as a site survey for IPOD and 1000 m contours of bathymetry. Location of Leg 67 drill sites and industry wells are shown by circles.
- Figure 2. A portion of records GUA-6 parallel to the strike of the trench in the mid-slope area showing the amplitude contrast between slope deposits and the top of the continental framework. This display was made without AGC and at a low gain to prevent clipping.
- Figure 3. Bathymetric map at 200 m contour interval from University of Texas data. Area A at the foot of the slope has a trend that may reflect the collision of a large ridge with the slope as explained in the text.
- Figure 4. Sections across the slope along seismic records showing the base of the slope deposits and prominent BSR's. Records 2 and 13 include parts of San Jose Canyon and the dashed line in 13 shows configuration of the seafloor along one side of the Canyon.
- Figure 5. Contours on the base of the slope deposits from all multichannel seismic data. Only the lines across the margin are shown. The contours begin at the edge of the slope and end at the trench axis. The irregularity of the mid-slope is generalized because of the wide spacing of ships tracks relative to the roughness of the topography.
- Figure 6. Part of GUA-28 across San Jose Canyon showing erosion. The prominent discontinuity on the left bank is the Oligo-Miocene unconformity.

Figure 7. Part of seismic record GUA-13 across the mid-slope where Site 496 was drilled and an interpretive line drawing showing the structure of the slope deposits and a base of gas hydrate BSR. The landward dipping reflection described by Ladd et al (this volume) is on the right.

Figure 8. Parts of records GUA-8 and 9 where coherent reflections from possible subducted strata are seen.

Figure 9. An example of polarity reversal between the water bottom and a strong BSR on GUA-14. Note the low amplitudes of reflections in the slope sediment above the BSR. Seismic traces are from Ladd et al, (this volume).

Figure 10. A diagram from Shipley et al, (1979), with the field containing 25 points from BSR's identified off Guatemala.

Figure 11. Thickness of slope deposits from the edge of the shelf to the trench axis.

Figure 12. Summary of temperature gradients measured in drill holes off Guatemala and those calculated from the depth of the base of gas hydrate BSR's. The temperature at 494 was measured in the hole for 1 month after drilling.

Figure 13. Unpublished temperature determinations from the Petral well corrected for drilling disturbances by the method of _____, (19). Gradients shown are those assumed for this study.

REFERENCES

- Aoki, Y. and Tamano, T. (1982) Detail structure of the inner trench slope of the Nankai Trough, from migrated seismic sections, Amer. Assoc. Pet. Geol. Memoir in press.
- Aubouin, J., Stephan, J. F., Renard, V., and Lonsdale, P., A Seabeam survey of the Leg 67 area (Mid America Trench off Guatemala) this volume.
- Azema, J. and Tournon, J., The Guatemala Margin, and the Nicoya Complex, and the origin of the Caribbean Plate, this volume.
- Boyce, R. E. (1976) Sound velocity-density parameters of sediment and rock from DSDP drill sites 315-318 on the Line Islands chain, Manihiki Plateau, and Tuamotu Ridge in the Pacific Ocean in Schlanger, S. O., Jackson, E. D., et al., Initial Reports of the Deep Sea Drilling Project, v. 33, Washington (U.S. Government Printing Office) p. 695-728.
- Cadet, J. P., Pouclet, A., Thisse, Y., Bardintzeff, J. M., and Azema, J., Middle America Neogene explosive volcanism and ash layers: evidence from Guatemala trench transect (DSDP Leg 67), this volume.
- Couch, R., and Woodcock, S., (1981), Gravity and structure of the continental margins of southwestern Mexico and northwestern Guatemala, J. Geophys. Res., v. 86, pp. 1829-1840.
- Hilde, T. W. C., and Sharman, G. F. (1978), Fault structure of the descending plate and its influence on the subduction process: EOS (Am Geophys. Union Trans.) v. 59, p. 1182.
- Ibrahim, A. K., Latham, G. V., and Ladd, J., 1979, Seismic refraction and reflection measurements in the Middle America Trench offshore Guatemala: in Ahrens, T. J., (ed.), Journal of Geophysical Research, v. 84, no. B 10, p. 5643-5649.

- Kennett, J., McBirney, A., and Thunell, R. (1977), Episodes of Cenozoic volcanism in the Circum-Pacific region, *Jour. Volcanol. Geother. Res.* 2, p. 145-163.
- Ladd, J. W., Ibrahim, A. K., McMillen, K. J., Latham, G. V., von Huene, R. E., Watkins, J. E., Moore, J. C., and Worzel, J. L., 1978, Tectonics of the Middle America Trench offshore Guatemala, in International Symposium of the Guatemala February 4, Earthquake and Reconstruction Process (held in Guatemala City, May 1978), v. 1.
- Ladd, J. W., and Schroder, S. C., The continental shelf off Guatemala: The seismic stratigraphy and structure of the forearc basin, this volume.
- Ladd, J. W., Ibrahim, A. K., McMillen, K. J., Latham, G. V., and von Huene, R. E., Interpretation of seismic reflection data of the Middle America Trench offshore Guatemala, this volume.
- Langseth, M., and T. Burch, 1980, Geothermal observations of the Japan trench transect: in Scientific Party, Initial Reports of the Deep Sea Drilling Project, 56, 57, pt. 2, Washington (U.S. Government Printing Office), p. 1207-1210.
- Moore, J. C., Watkins, J., Bachman, S. B., Beghtel, F. W., Butt, A., Didyk, B. M., Leggett, J., Lundberg, N., McMillen, K. J., Niitsuma, N., Shepard, L. E., Shipley, T. H., Stephan, J. F., Stradner, H., 1979, The Middle America Trench off Mexico: in Cochran, W., (ed.) Geotimes, v. 24, no. 9, p. 20-22.
- Schweller, W. J., and Kulm, L. D., 1978, Extensional rupture of oceanic crust in the Chile Trench: *Marine Geology*, v. 28, p. 271-291.
- Scientific Staff, Site 494 this volume.
- Scientific Party, Sites 499 and 500 this volume

Seely, D. R., Vail, P. R., and Walton, G. G., 1974, Trench slope model, in
Geology of Continental Margins, Burk, C. A., and Drake, C. L., (eds.)
Springer-Verlag, New York, p. 261-283.

Seely, D., 1979, Geophysical investigations of continental slopes and rises:
in Watkins, J. S., and Montadert, L., eds., Geological and Geophysical
Investigation of Continental Margins: Tulsa, OK, Am. Assoc. of Pet. Geo.
Memoir 51.

Shipley, T. H., Houston, M. H., Buffler, R. T., Shaub, F. J., McMillen, K. J.,
Ladd, J. W., and Worzel, J. L. (1979), Seismic evidence of widespread
possible gas hydrate horizons on continental slopes and rises: Am.
Assoc. of Pet. Geo. Bulletin v. 63, p. 2204-2213.

Shor, G. G., and Fisher, R. L., (1961), Middle America Trench: Seismic
refraction studies, Geol. Soc. Amer. Bull. 72, p. 721-730.

von Huene, R., J. Aubouin, J. Azema, G. Blackinton, J. A. Carter, W. T.
Coulbourn, D. S. Cowan, J. A. Curiale, C. A. Dengo, R. W. Faas, W.
Harrison, R. Hesse, D. M. Husson, J. W. Ladd, N. Muzylov, T Shiki, P. R.
Thompson and J. Westberg, 1980, Leg 67: The Deep Sea Drilling Project
Mid-America Trench transect off Guatemala: Geol. Soc. of Amer. Bull.,
v. 91, p. 421-432.

FIGURE CAPTIONS

- Figure 1. Ships tracks of multichannel seismic reflection records made in 1977 by the University of Texas as a site survey for IPOD and 1000 m contours of bathymetry. Location of Leg 67 drill sites and industry wells are shown by circles.
- Figure 2. A portion of records GUA-6 parallel to the strike of the trench in the mid-slope area showing the amplitude contrast between slope deposits and the top of the continental framework. This display was made without AGC and at a low gain to prevent clipping.
- Figure 3. Bathymetric map at 200 m contour interval from University of Texas data. Area A at the foot of the slope has a trend that may reflect the collision of a large ridge with the slope as explained in the text.
- Figure 4. Sections across the slope along seismic records showing the base of the slope deposits and prominent BSR's. Records 2 and 13 include parts of San Jose Canyon and the dashed line in 13 shows configuration of the seafloor along one side of the Canyon.
- Figure 5. Contours on the base of the slope deposits from all multichannel seismic data. Only the lines across the margin are shown. The contours begin at the edge of the slope and end at the trench axis. The irregularity of the mid-slope is generalized because of the wide spacing of ships tracks relative to the roughness of the topography.
- Figure 6. Part of GUA-28 across San Jose Canyon showing erosion. The prominent discontinuity on the left bank is the Oligo-Miocene unconformity.

- Figure 7. Part of seismic record GUA-13 across the mid-slope where Site 496 was drilled and an interpretive line drawing showing the structure of the slope deposits and a base of gas hydrate BSR. The landward dipping reflection described by Ladd et al (this volume) is on the right.
- Figure 8. Part of record GUA 9 where coherent reflections from possible subducted sediment are seen.
- Figure 9. An example of polarity reversal between the water bottom and a strong BSR on GUA-14. Note the low amplitudes of reflections in the slope sediment above the BSR. Seismic traces are from Ladd et al, (this volume).
- Figure 10. A diagram from Shipley et al, (1979), with the field containing 25 points from BSR's identified off Guatemala.
- Figure 11. Thickness of slope deposits from the edge of the shelf to the trench axis.
- Figure 12. Summary of temperature gradients measured in drill holes off Guatemala and those calculated from the depth of the base of gas hydrate BSR's. The temperature at 494 was measured in the hole for 1 month after drilling.
- Figure 13. Unpublished temperature determinations from the Petrel well corrected for drilling disturbances by the method of _____, (19). Gradients shown are those assumed for this study.

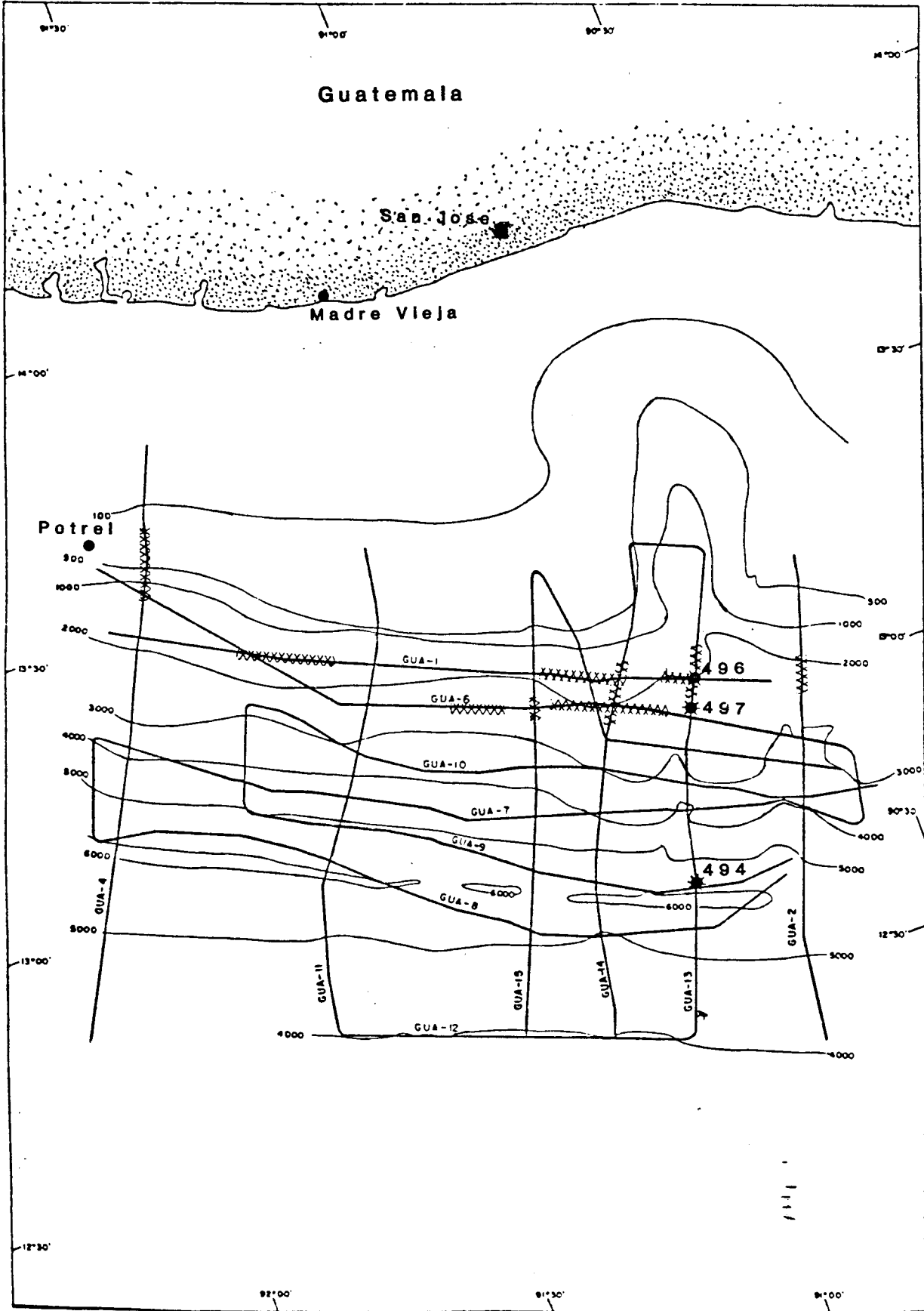
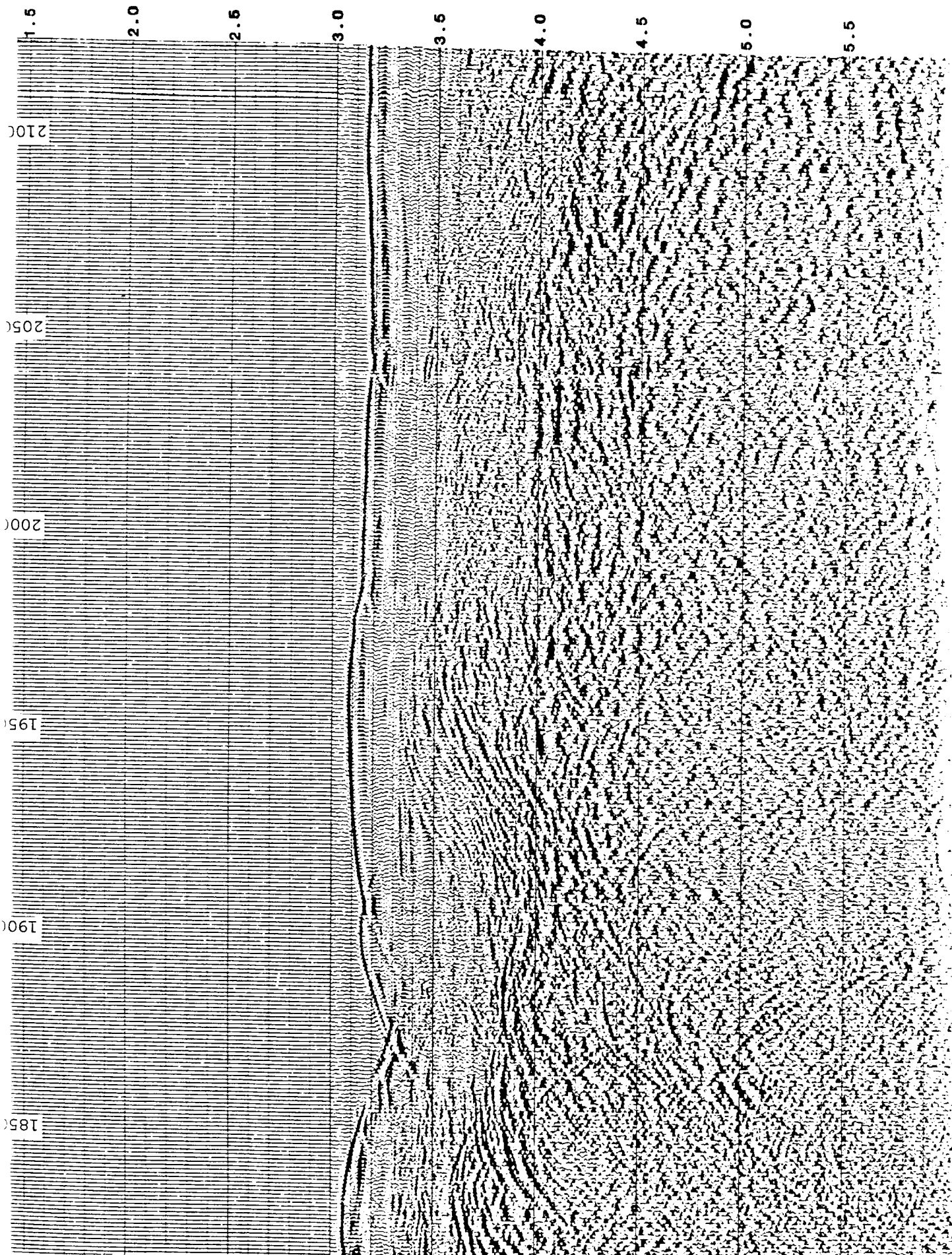
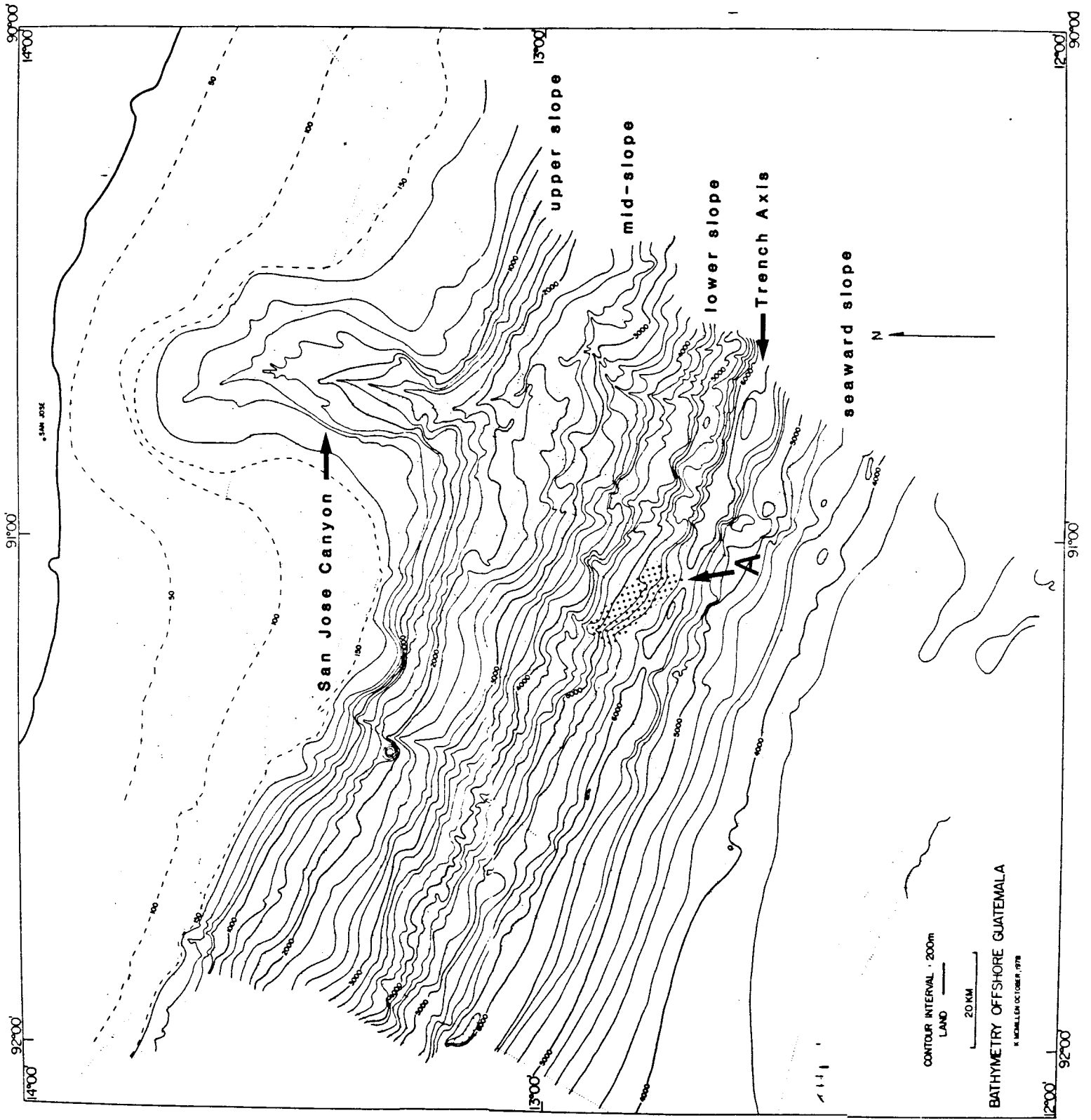


FIG. 1

TWO WAY TRAVEL (Sec)





CONTOUR INTERVAL: 200m

LAND

20 KM

BATHYMETRY OFFSHORE GUATEMALA

1:100,000 OCTOBER, 1978

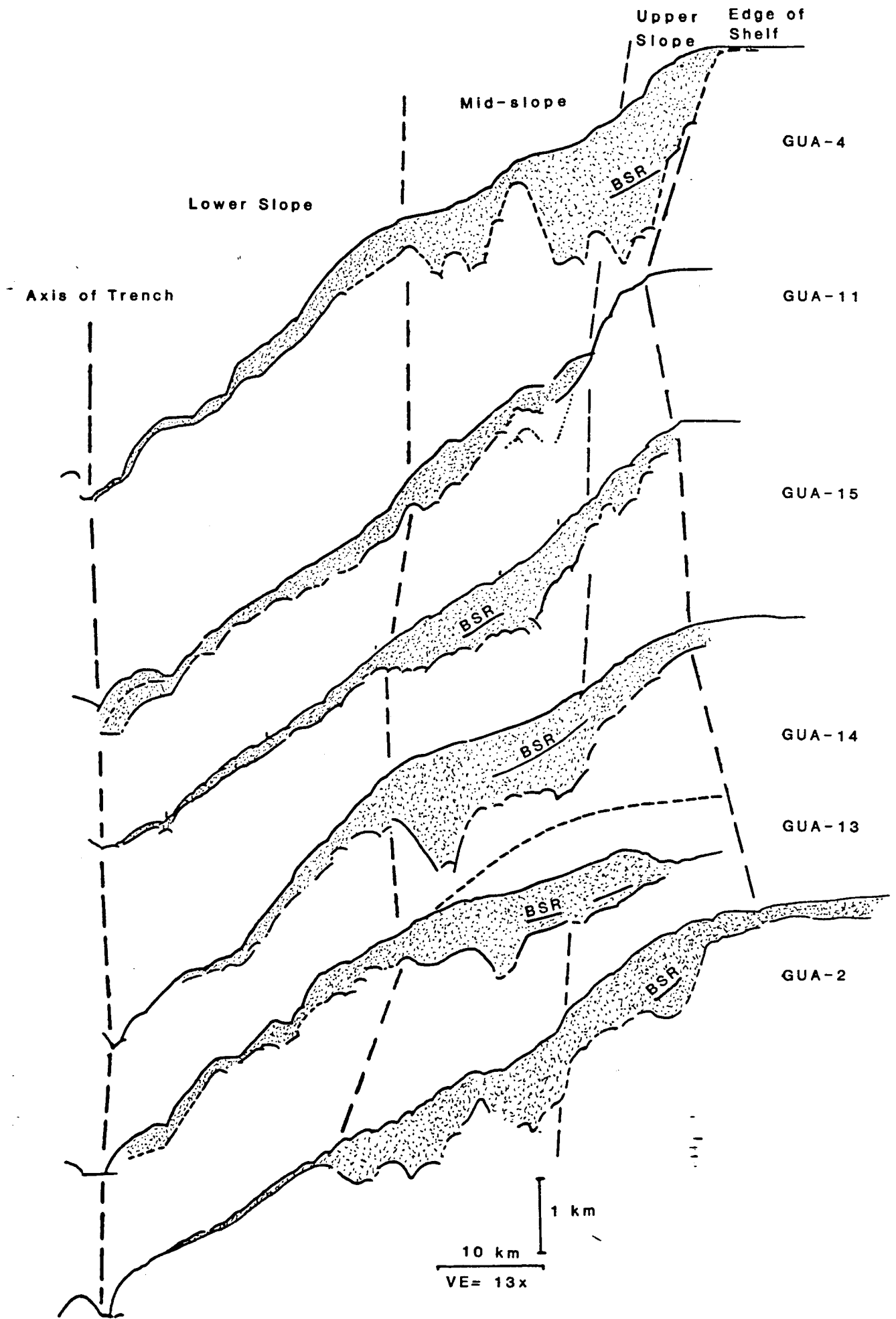


Fig. 4

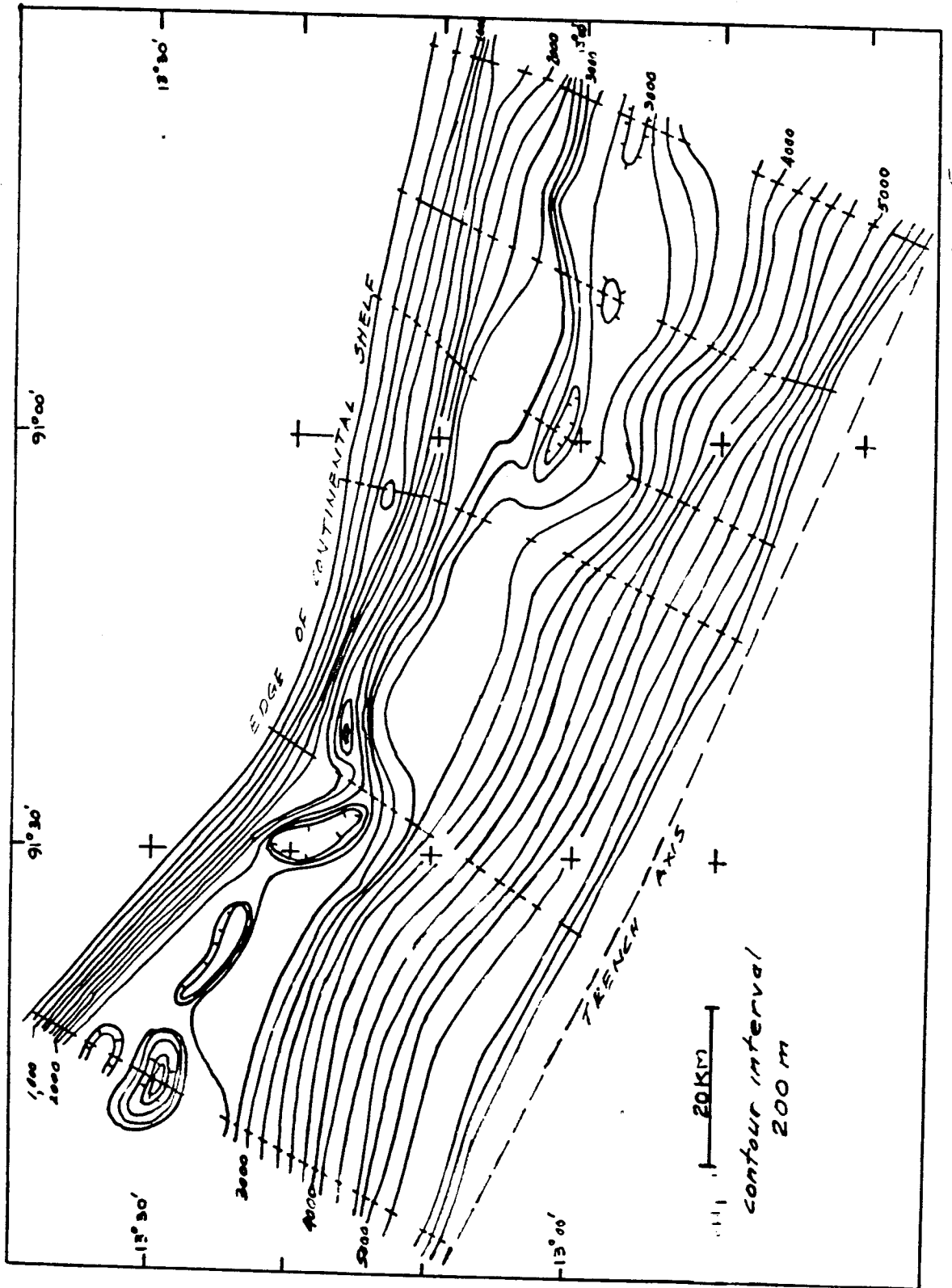
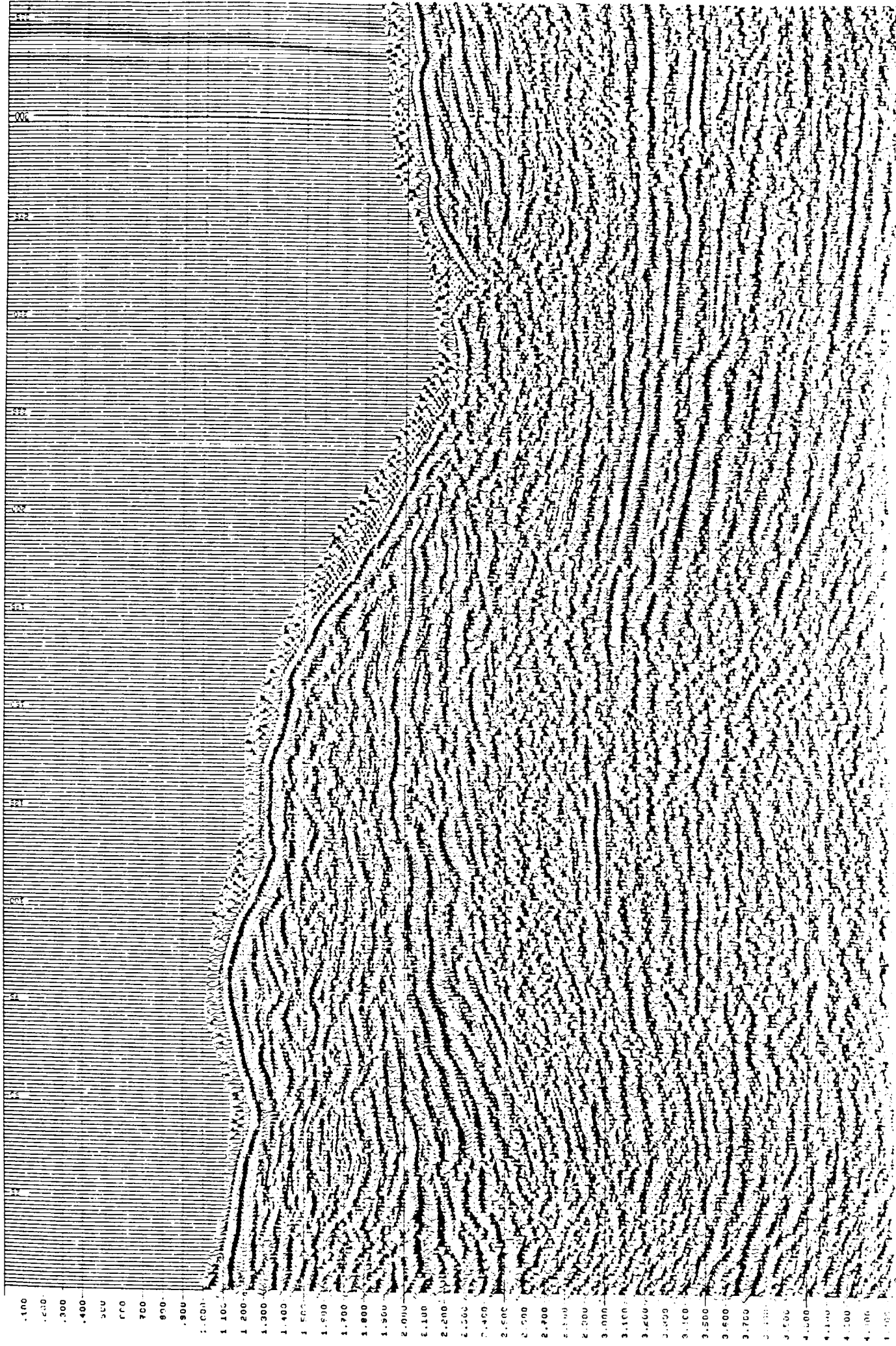
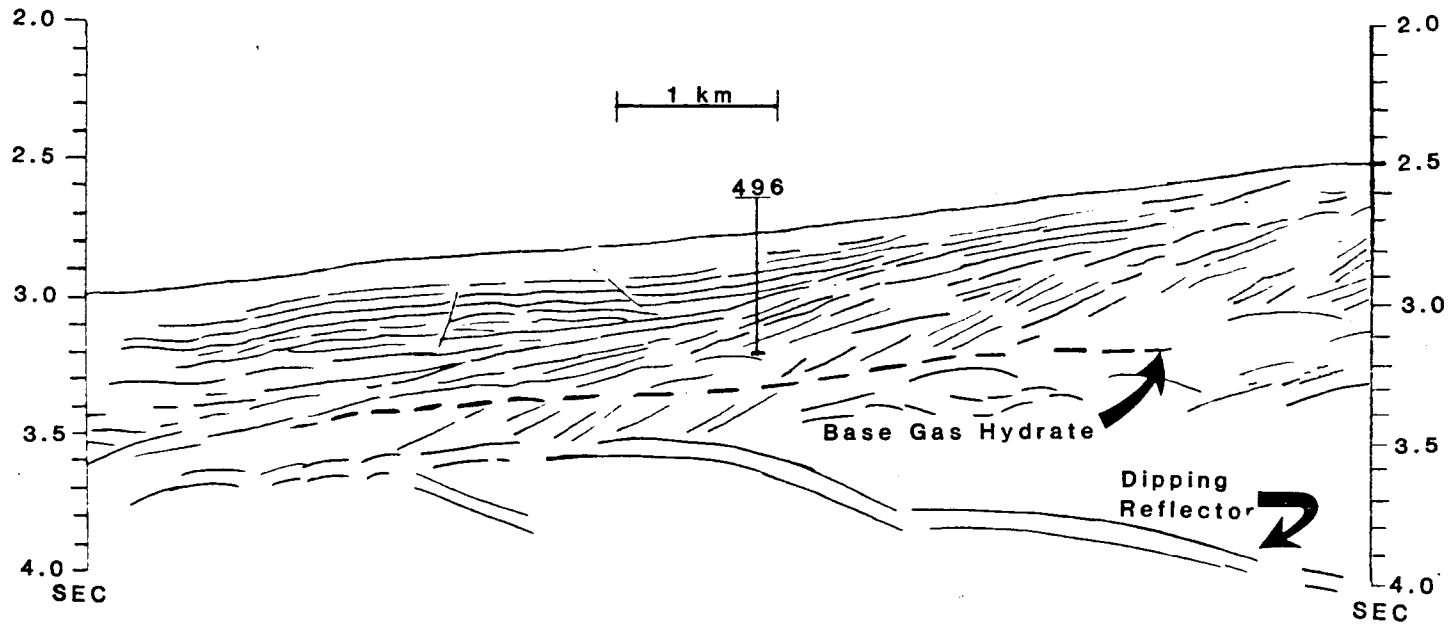
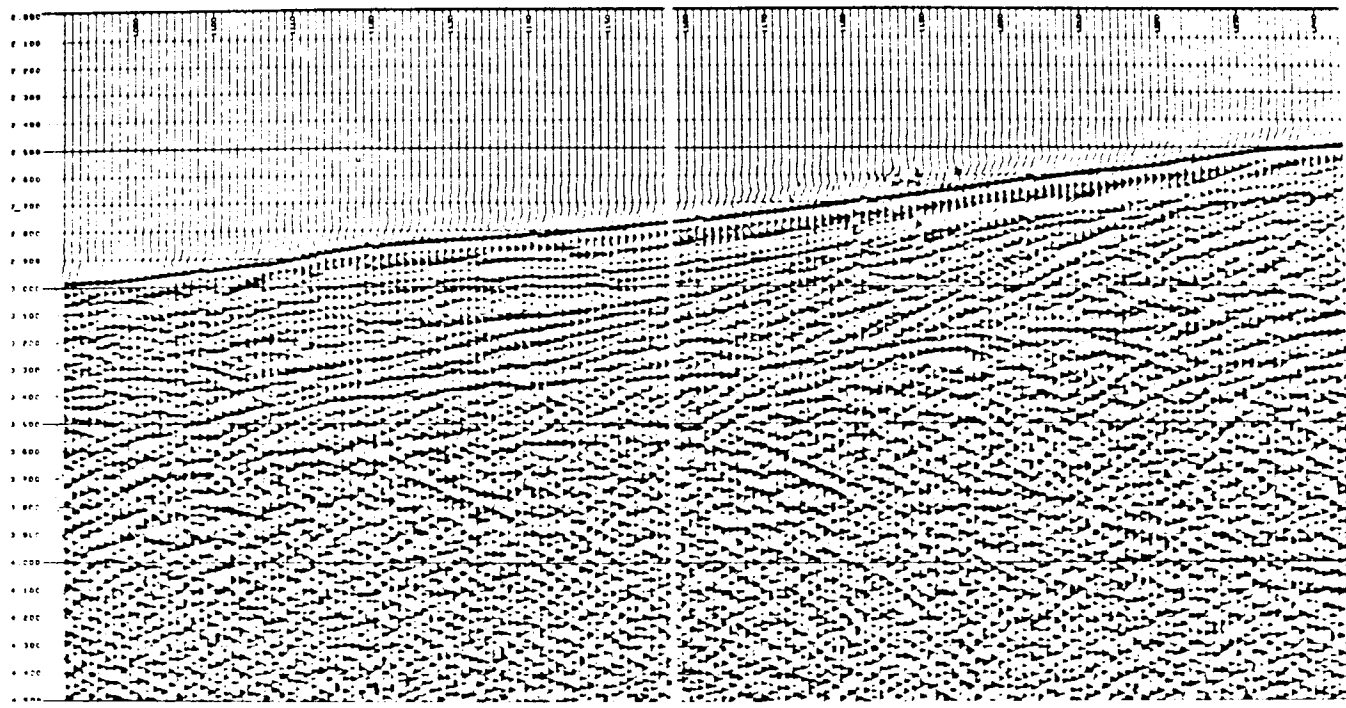
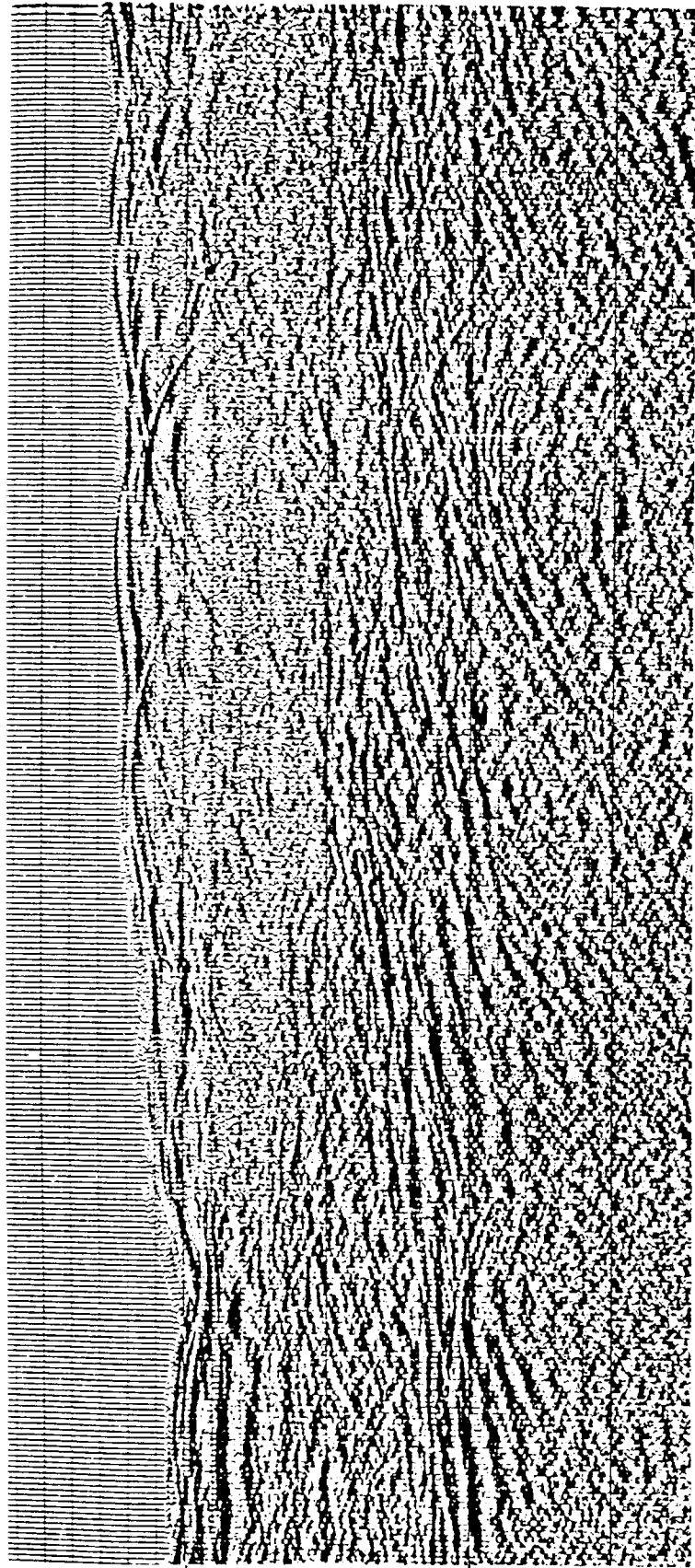


FIG 5



0.100
0.200
0.300
0.400
0.500
0.600
0.700
0.800
0.900
1.000
1.100
1.200
1.300
1.400
1.500
1.600
1.700
1.800
1.900
2.000
0.000
0.100
0.200
0.300
0.400
0.500
0.600
0.700
0.800
0.900
1.000
1.100
1.200
1.300
1.400
1.500
1.600
1.700
1.800
1.900
2.000
2.100
2.200
2.300
2.400
2.500
2.600
2.700
2.800
2.900
3.000
3.100
3.200
3.300
3.400
3.500
3.600
3.700
3.800
3.900
4.000
4.100
4.200
4.300
4.400





SECONDS
0
5

GLIA 9

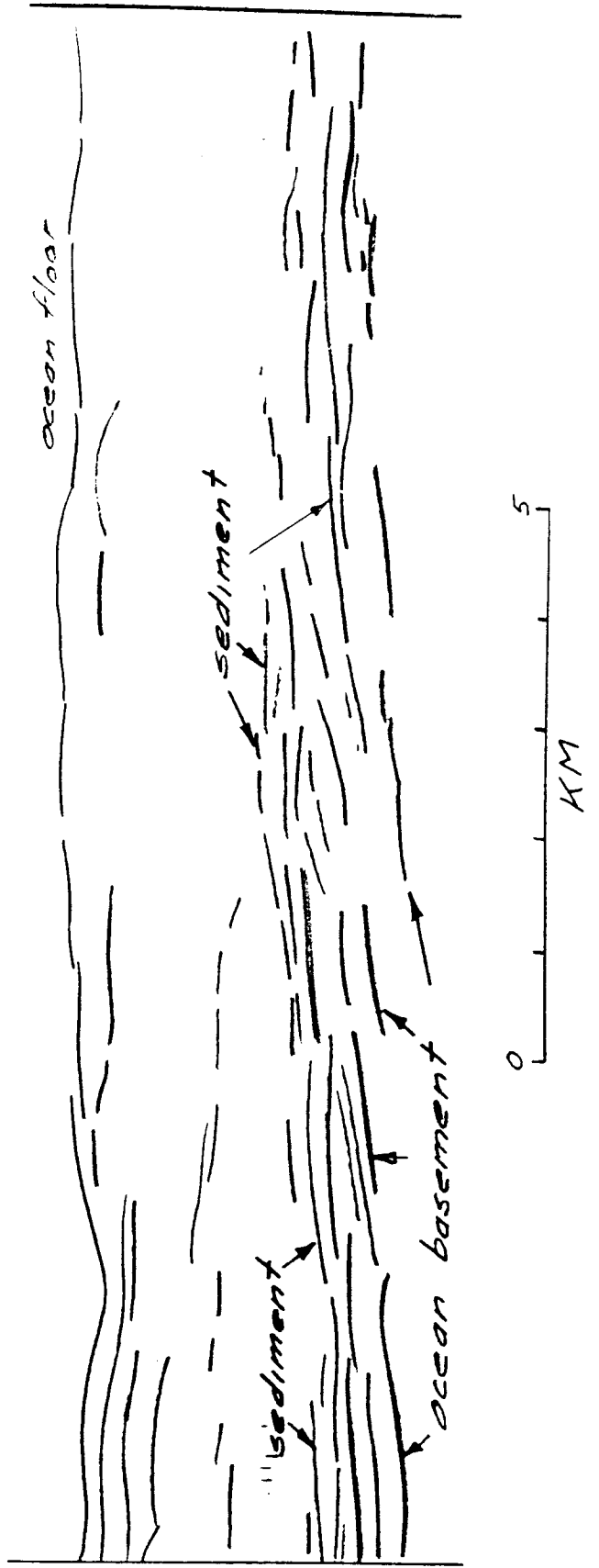
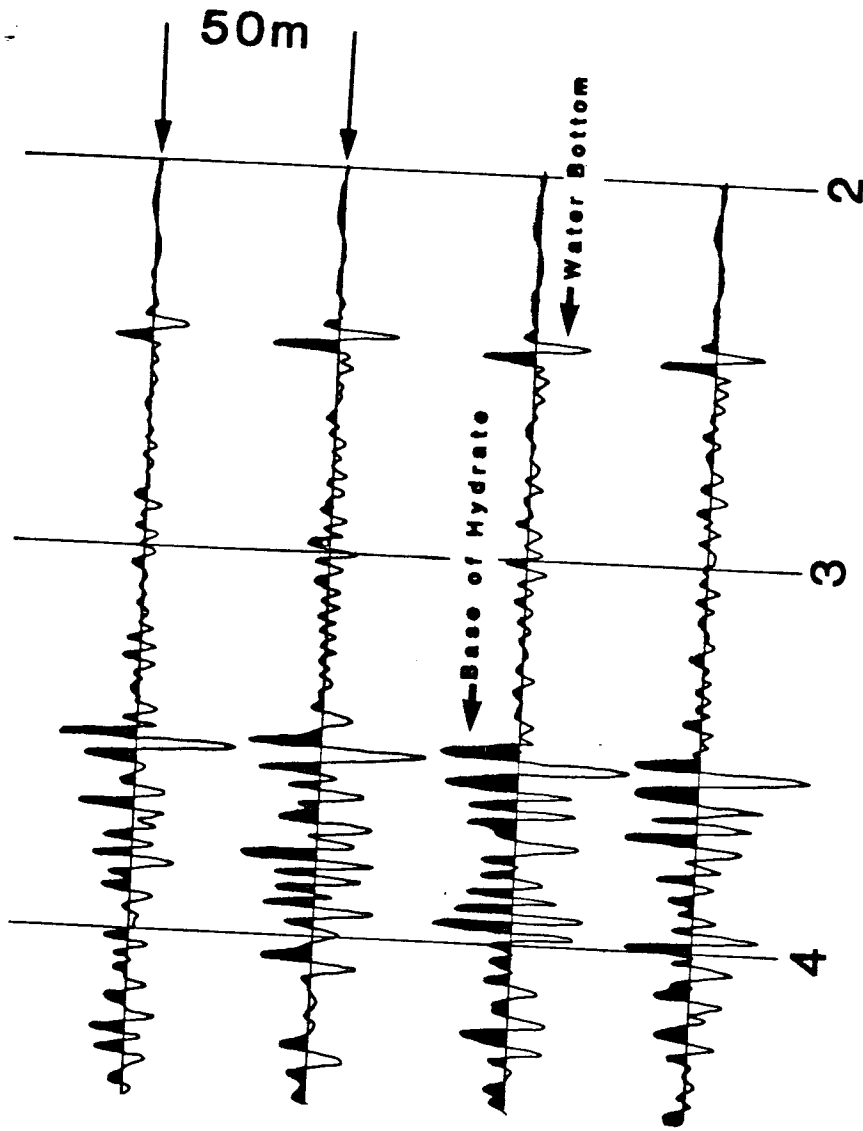


Fig. 8



Two Way Travel (sec)

